

1 **Supplementary Material**

2

3 Figure S1. CAR T_{N/SCM} are less differentiated and display a reduced exhausted-like status *in vitro*.

4 Figure S2. CAR T_{N/SCM} expand more in HuSGM3 mice without causing detrimental side effects.

5 Figure S3. CAR T_{N/SCM} and CAR T_{BULK} are effective *in vivo* and equally represented in the meta-
6 cluster analysis.

7 Figure S4. CAR T_{N/SCM} are less prone to cause multifocal brain hemorrhages *in vivo*.

8 Figure S5. CAR T_{N/SCM} BBz display lower activation *in vitro* and expand more *in vivo*.

9 Figure S6. CAR T_{N/SCM} activate less upon leukemia encounter *in vitro*.

10 Figure S7. Milder activation status characterizes CAR T_{N/SCM} in the presence of myeloid cells.

11 Figure S8. CAR T_{N/SCM} better calibrate monocyte-like activation and cytokine production.

12

13

14

15

16

17

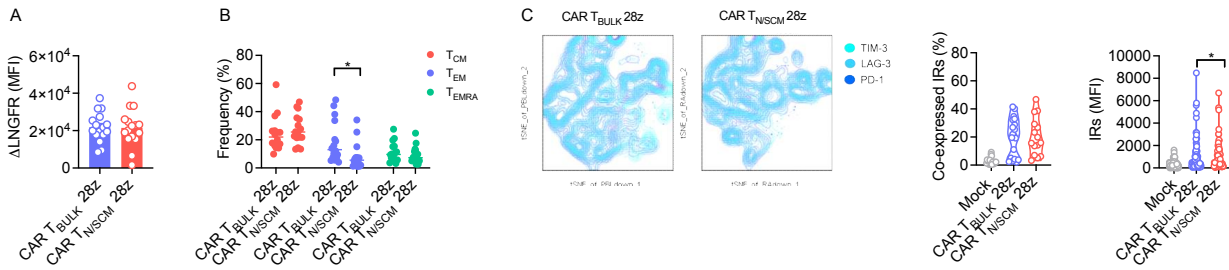
18

19

20

21

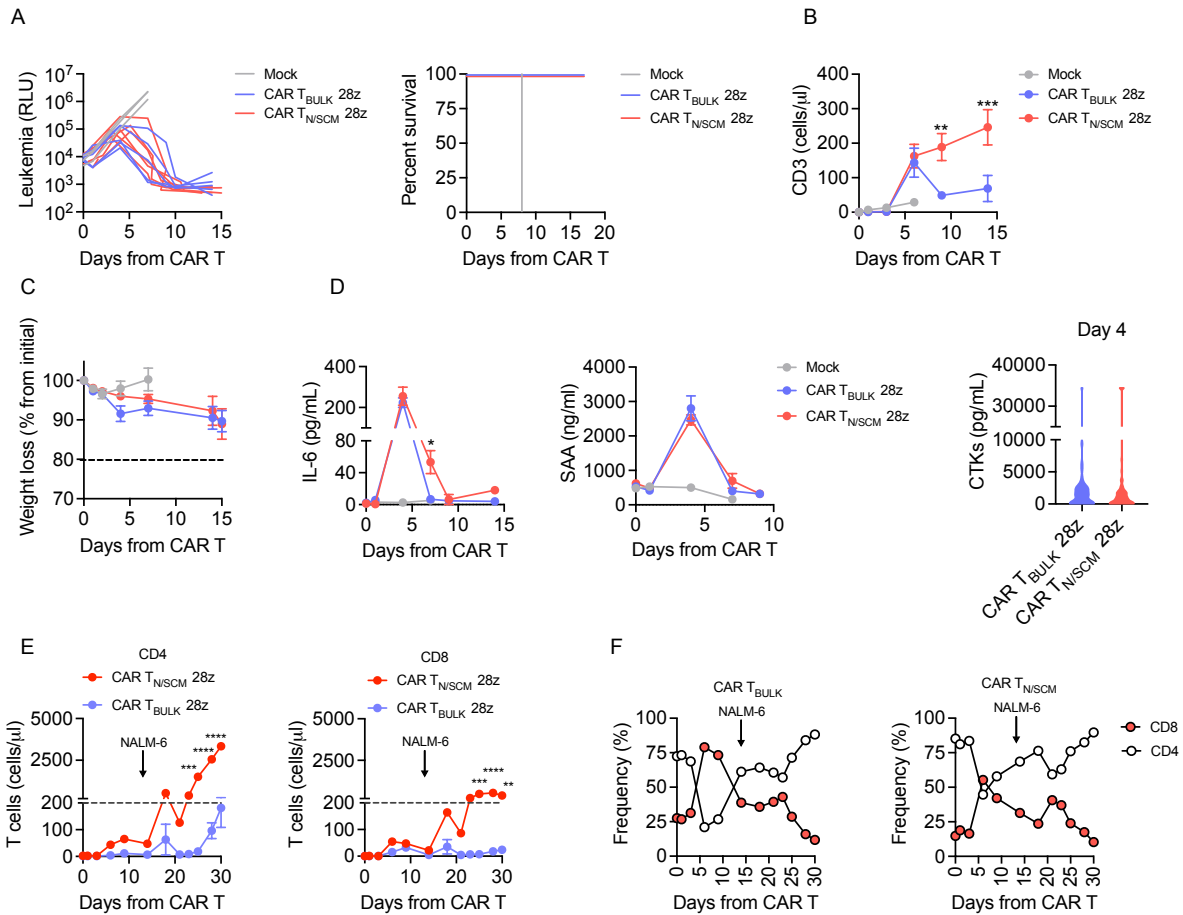
22



23

24 **Figure S1. CAR T_{N/SCM} are less differentiated and display a reduced exhausted-like status *in***
 25 ***vitro***

26 **A)** ΔLNGFR marker expression reported as MFI at the end of culture protocol (n=16). **B)** Frequency
 27 of central memory, effector memory and terminally differentiated T-cell subsets at the end of culture
 28 (n=16). **C)** Left plots and panel: Tsne representation and percentage of T cells co-expressing TIM-3,
 29 LAG-3 and PD-1 inhibitory receptor (IRs) after co-culture with CD19+ targets (NALM-6 and ALL-
 30 CM cell lines; n=19 for CAR T_{BULK}, n=15 for CAR T_{N/SCM}). Right panel: IRs mean fluorescence
 31 intensity (MFI) values (n=11 donors). Data are represented as the result of mean ±SEM together with
 32 overlapping scattered values and box and violin plots. Results of two-way ANOVA (B) and paired t-
 33 test (A, C) are reported when statistically significant (*p<0.05).



34

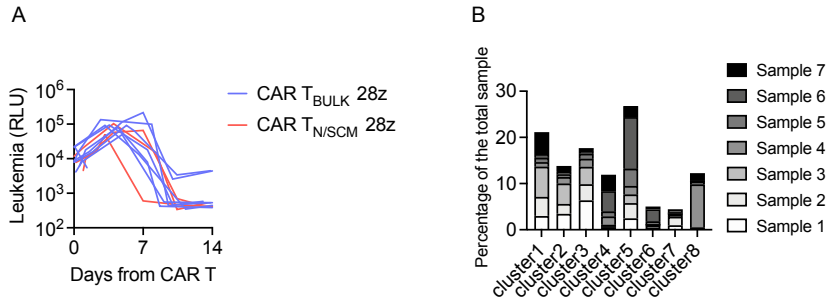
35

36 **Figure S2. CAR T_{N/SCM} expand more in HuSGM3 mice without causing detrimental side effects**

37 HuSGM3 mice were infused with Lucia⁺/NGFR⁺/NALM-6 cells and treated with 3×10^6 CAR
 38 T_{N/SCM} (n=6), CAR T_{BULK} (n=5) or Mock control (n=3) and analyzed for antitumor activity and toxic
 39 manifestations. **A)** Left: Bioluminescence detection of tumor growth after treatment. Data are
 40 represented as single interspersed lines representing individual treated mice. Right: Kaplan–Meyer
 41 survival analysis of mice. **B)** T-cell expansion in the peripheral blood of mice. **C, D)** Evaluation of
 42 signs and symptoms typical of CRS development in HuSGM3 leukemia bearing mice, represented
 43 by weight loss (**C**) and serum levels of IL-6 (**D**, left), murine serum amyloid A (SAA, **D** middle) and
 44 other pro-inflammatory cytokines, namely IL-10, TNF- α , IL-1 α , IFN- γ , MIP-1 α , IP-10, MCP-1, IL-
 45 8, IL-2 and again IL-6 (**D**, right). **E)** CD4 (left) and CD8 (right) T-cell expansion within CAR T_{BULK}
 46 (n=17) and CAR T_{N/SCM} (n=17) in the peripheral blood of NALM-6 bearing mice measured at

47 different time points after treatment. **F)** CD4 and CD8 frequency in CAR T_{BULK} (left) and CAR T_{N/SCM}
48 (right) measured in the peripheral blood of NALM-6 bearing mice at different time points after
49 treatment. Data are represented as the result of mean \pm SEM and box and violin plots. Results of
50 unpaired t-test (**D**, right panel) and two-way ANOVA (**A-F**) are reported when statistically significant
51 (* $p < 0.05$; ** $p < 0.01$; *** $p < 0.001$).

52



53

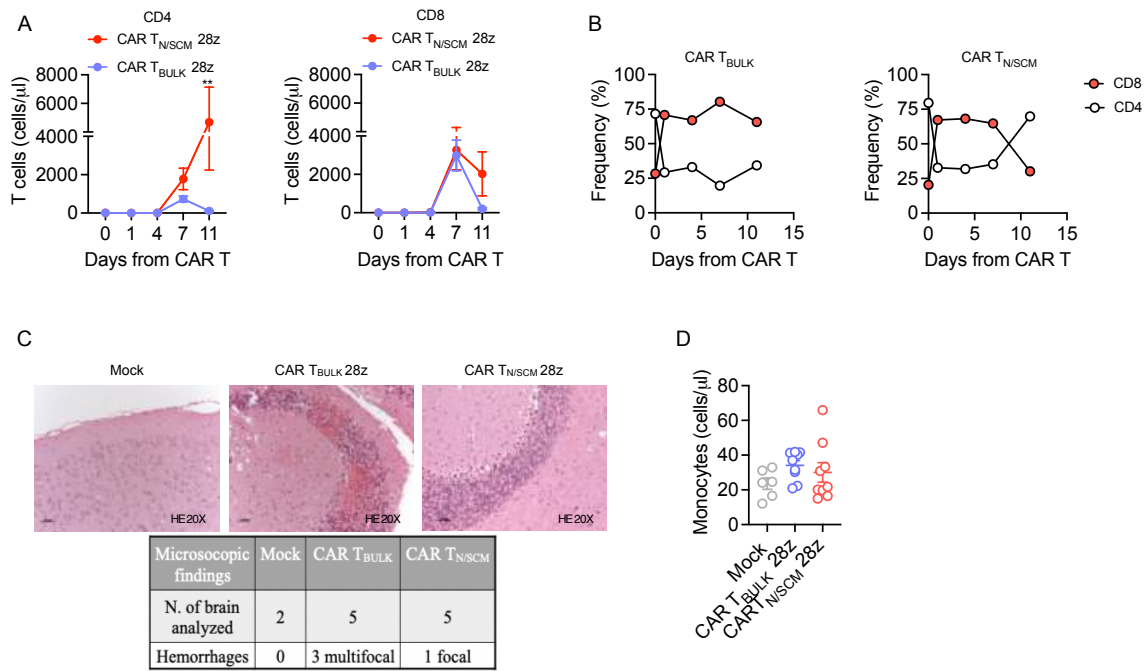
54

55 **Figure S3. CAR T_{N/SCM} and CAR T_{BULK} are effective *in vivo* and equally represented in the**
 56 **meta-cluster analysis**

57 **A)** Bioluminescence detection of Lucia+/NGFR+/NALM-6 systemic growth in HuSGM3 mice after
 58 treatment with 1×10^6 CAR T_{N/SCM}, CAR T_{BULK} or Mock control. Data are represented as single
 59 interspersed lines representing individual treated mice (n=7 for CAR T_{BULK} and n=3 for CAR T_{N/SCM}).

60 **B)** Distribution of each sample in the relevant clusters after BH-SNE analysis.

61



62

63

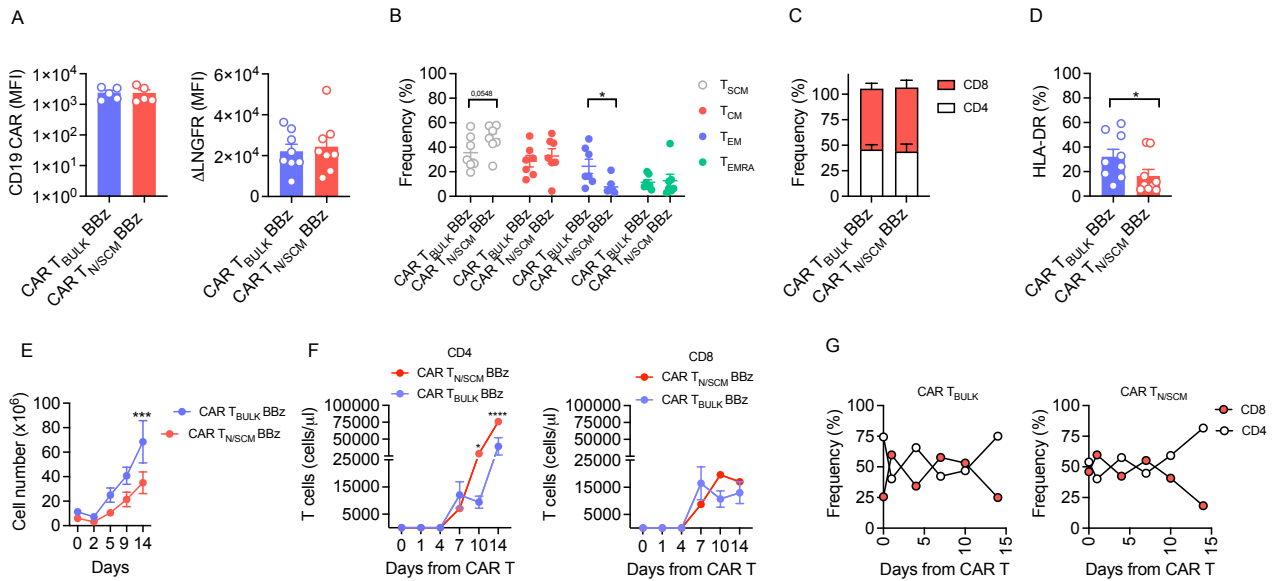
64 **Figure S4. CAR T_{N/SCM} are less prone to cause multifocal brain hemorrhages *in vivo***

65 **A)** CD4 (left) and CD8 (right) T-cell expansion within CAR T_{BULK} (n=6) and CAR T_{N/SCM} (n=6) in
 66 the peripheral blood of NALM-6 bearing mice measured at different time points after treatment. **B)**
 67 CD4 and CD8 frequency in CAR T_{BULK} (left) and CAR T_{N/SCM} (right) measured in the peripheral
 68 blood of NALM-6 bearing mice at different time points after treatment. **C)** Hematoxylin and eosin-
 69 stained section of brains belonging to representative Mock control, CAR T_{BULK} and CAR T_{N/SCM}
 70 treated mice (20x magnification; bar:50 micron) with relative incidence table of microscopic findings
 71 recorded in collected brains belonging to HuSGM3 leukemia-bearing mice treated with CD28-
 72 costimulated CAR T_{N/SCM}, CAR T_{BULK} and Mock control. **D)** Monocyte absolute number
 73 immediately before CAR T-cell infusion in HuSGM3 leukemia bearing mice (n=9 for CAR T_{BULK},
 74 n=9 for CAR T_{N/SCM}, n=6 for Mock).

75

76

77

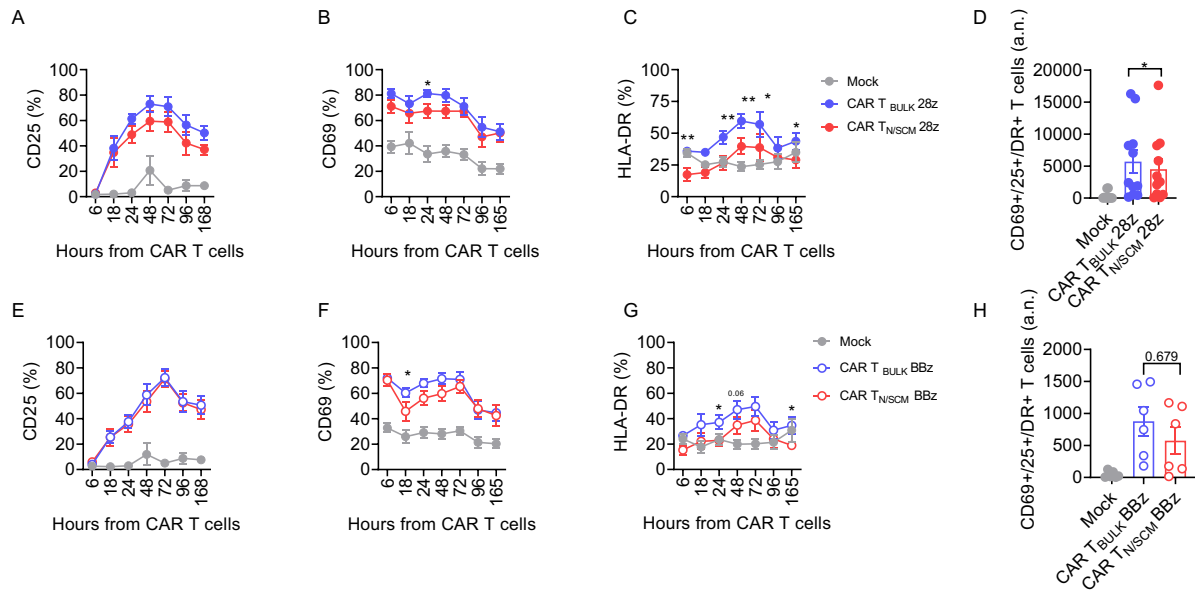


78

79 **Figure S5. CAR T_{N/SCM} BBz display lower activation *in vitro* and expand more *in vivo***

80 **A)** CD19.CAR scFv (n=5, left) and Δ LINGFR marker gene (n=8, right) expressed as MFI at the end
 81 of culture protocol. **B)** Memory phenotype at the end of T-cell manufacturing (n=7 donors). **C)**
 82 CD4/CD8 ratio (n=9 donors) and **D)** HLA-DR expression at the end of culture (n=9 donors). **E)** Fold
 83 expansion at different time points during culture (n=7). **F)** CD4 (left) and CD8 (right) T-cell
 84 expansion of CAR T_{BULK} (n=13) and CAR T_{N/SCM} (n=12) in the peripheral blood of NALM-6 bearing
 85 mice measured at different time points after treatment. **G)** CD4 and CD8 frequency of CAR T_{BULK}
 86 (left) and CAR T_{N/SCM} (right) measured in the peripheral blood of NALM-6 bearing mice at different
 87 time points after treatment. Data are represented as the result of mean \pm SEM together with
 88 overlapping scattered values. Results of paired t-tests (C) and two-way ANOVA (A, B, D) are
 89 reported when statistically significant (*p<0,05; ***p<0,001).

90

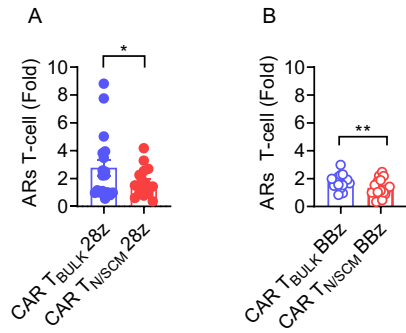


91

92 **Figure S6. CAR T_{N/SCM} activate less upon leukemia encounter *in vitro***

93 Activation kinetic of CAR T cells at different time points after stimulation with NALM-6 cells
 94 measured as upregulation of **A, E**) CD25 activation marker, **B, F**) CD69 activation marker and **C, G**)
 95 HLA-DR activation marker expression (CAR T_{BULK}/CAR T_{N/SCM} 28z n=11; CAR T_{BULK}/CAR T_{N/SCM}
 96 BBz n=11). **D, H**) Number of T cells co-expressing CD25/CD69/HLA-DR activation markers 48
 97 hours after co-culture with tumor cells (n=11). Data are represented as the result of mean ±SEM
 98 together with overlapping scattered values and results of paired t-test is reported when statistically
 99 significant (*p<0,05).

100



101

102

103 **Figure S7. Milder activation status characterizes CAR T_{N/SCM} in the presence of myeloid cells**

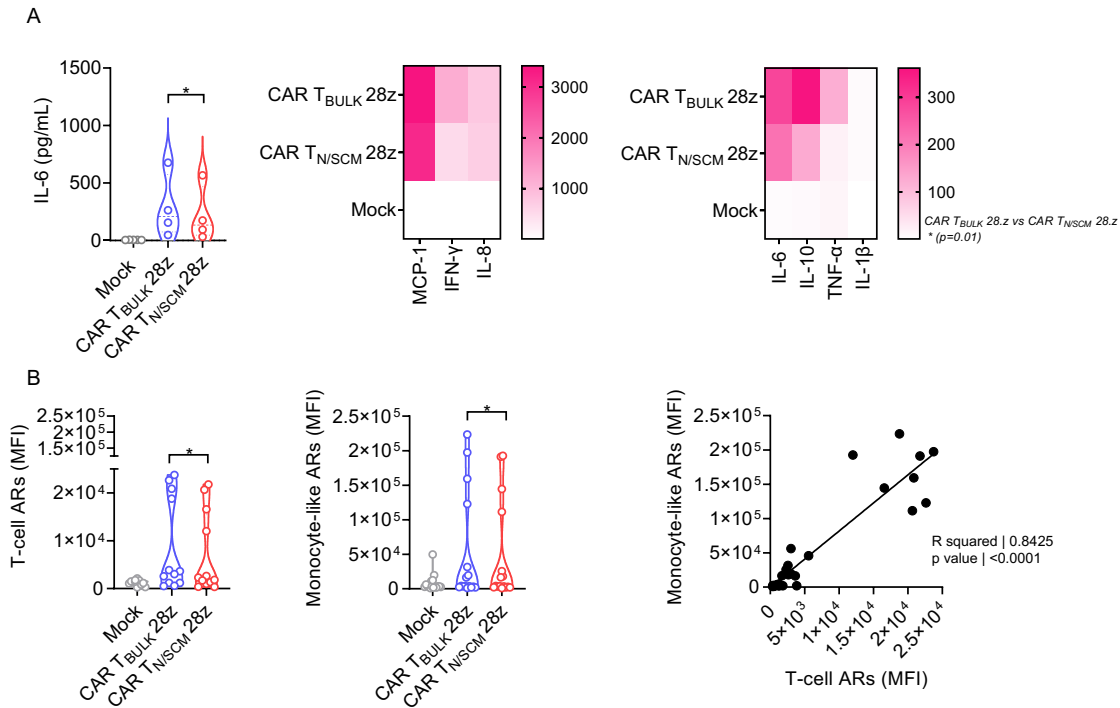
104 Activation receptors (ARs) upregulation on **A)** CD28 and **B)** 4-1BB co-stimulated CAR T cells

105 (CD54/CD86/HLA-DR/CD25) expressed as fold 24 hours after plating a tripartite coculture

106 comprising NALM-6, CAR T cells and autologous monocyte (CAR T_{BULK}/CAR T_{N/SCM} 28z n=5;

107 CAR T_{BULK}/CAR T_{N/SCM} BBz n=4).

108



109

110 **Figure S8. CAR T_{N/SCM} better calibrate monocyte-like activation and cytokine production**

111 CAR T_{BULK} and CAR T_{N/SCM} were cultured with NALM-6 and THP-1 cells. **A**) IL-6 production (left
 112 panel) and heat-map visualization of cytokine release (right panel) 24 hours after plating (n=4). **B**)
 113 Activation receptors (ARs) upregulation on T cells (CD54/CD86/HLA-DR, left) and THP-1 cells
 114 (CD54/CD86/CD163/HLA-DR, middle) expressed as MFI 24 hours after plating, together with
 115 correlation analysis between T-cell and THP-1 activation states (considering CD54/CD86/HLA-DR,
 116 right; n=4).